Effect of curvature on cholesteric liquid crystals in toroidal geometries

Ana R. Fialho,[*] Nelson R. Bernardino,[†] Nuno M. Silvestre,[‡] and Margarida M. Telo da Gama
Departamento de Física da Faculdade de Ciências, Centro de Física Teórica e Computacional, Universidade de Lisboa, P-1649-003 Lisboa, Portugal

(Received 25 August 2016; revised manuscript received 12 December 2016; published 17 January 2017)

The confinement of liquid crystals inside curved geometries leads to exotic structures, with applications ranging from biosensors to optical switches and privacy windows. Here we study how curvature affects the alignment of a cholesteric liquid crystal. We model the system on the mesoscale using the Landau-de Gennes model. Our study was performed in three stages, analyzing different curved geometries from cylindrical walls and pores, to toroidal domains, in order to isolate the curvature effects. Our results show that the stresses introduced by the curvature influence the orientation of the liquid crystal molecules, and cause distortions in the natural periodicity of the cholesteric that depend on the radius of curvature, on the pitch, and on the dimensions of the system. In particular, the cholesteric layers of toroidal droplets exhibit a symmetry breaking not seen in cylindrical pores and that is driven by the additional curvature.

DOI: 10.1103/PhysRevE.95.012702

I. INTRODUCTION

Liquid crystals (LCs) have dominated the display industry for over 50 years and are of standard use in small everyday devices [1–3]. Typically, such technology comprises a nematic LC confined between two flat plates, as in monitors [4,5], or encapsulated to cavities dispersed in a polymer matrix (PDLC), as in privacy windows [6–8]. These rely on the fact that LCs are fluid flexible media extremely sensitive to the confining surfaces and to applied external perturbations.

Nematics are the simplest of the LC phases. They differ from the isotropic phase by exhibiting long-range orientational order, which makes it energetically favorable for the nematic molecules to be (on average) uniformly aligned. In the presence of frustration, e.g., imposed by confinement, the nematic induces the nucleation of topological defects (in the orientational field) [9,10]. These are small regions of reduced orientational order that scale with the correlation length and play a major role in wetting [11], phase transitions [10], and in the interaction of colloidal particles dispersed in an LC [12]. Their nucleation is particularly important in the physics of bistable LC devices used in a large scale to indicate the price of any produce at your local supermarket [13].

Also with a wide range of applications are cholesteric LCs. From the macroscopic point of view, they differ from nematics by the fact that they exhibit spontaneous twist that, on the microscopic level, is the result of being composed of chiral molecules [9,10]. To the general public they are probably better known for their application as mood rings and thermometer strips [14,15] and eWriters [16]. A key feature of cholesteric LCs important for applications is the ability to control the reflected light by manipulating its spontaneous pitch, either by the application of external fields or by changing the temperature of the LC. This seems to be completely understood from the point of view of cholesterics confined to flat surfaces. However, as the display technology moves toward softer hardware it is of crucial importance to understand what is the effect of curvature on the cholesteric pitch.

The development of new soft-lithographic techniques made possible the controlled production of new PDLC matrices with droplets of prescribed shapes and nontrivial topologies [17]. Of particular interest are toroidal shapes, for which the Poincaré-Hopf theorem dictates that the net charge of the bulk defects is $\sum_i q_i = 0$, in the absence of surface defects. For a torus on the micrometer scale defects may appear in pairs of opposite charge [17]. However, as the system size increases the presence of topological defects becomes energetically unstable, and for a torus on the millimeter scale, the LC texture is completely free from topological defects as the LC has other alternatives to accommodate the orientational frustration [18]. Nonetheless, in some toroidal geometries the liquid crystal texture may exhibit defects. This happens when two regions of the confining surface have different boundary conditions [19], as observed in liquid crystal droplets adsorbed at micrometer fibers [20,21]. In cholesterics, however, the geometrically induced frustration can be accommodated by the formation of nonsingular disclinations (defects), with constant orientational order, rather than through the usual singular defects [22,23].

In this work we are interested in understanding what is the role of curvature on the texture of cholesteric liquid crystals confined to toroidal domains. This manuscript is organized in the following manner. In the next section we describe how we model the liquid crystal and briefly describe our numerical methods. To achieve our aim we have divided our study into three stages, which are presented in Sec. III. First, we consider a cholesteric liquid crystal in contact with a cylindrical substrate and analyze how the cholesteric is affected by decreasing the radius (increasing the curvature) of the cylindrical wall. In particular we show how adding curvature changes the local periodicity of the cholesteric as a response to emerging bend deformations. Second, we consider that the cholesteric is confined to a cylindrical pore and revisit some of the results obtained by Ambrozic and Žumer [24,25]. Finally, we consider the case of a toroidal domain and analyze how the curvature of the confining surface affects the cholesteric texture. We summarize our results in Sec. IV.

[*]Current address: School of Physics and Astronomy, University of Edinburgh, Peter Guthrie Tait Road, Edinburgh EH9 3FD, UK.
[†]Current address: Haitong Bank, S.A., Rua Alexandre Herculano, 38, P-1269-180 Lisboa, Portugal.
[‡]nmsilvestre@fc.ul.pt

II. MODEL

We use the Landau-de Gennes model to describe the cholesteric LC [9]. The order parameter is a traceless, symmetric second-rank tensor $\mathbf{Q}$ that carries information on the local average molecular orientation, the director field $\mathbf{n}$, and on the degree of orientational order S; for uniaxial nematics it takes the form $Q_{ij} = S(3n_i n_j - \delta_{ij})/2$, where δ_{ij} is the Kronecker δ. The free energy is written in invariant terms of $\mathbf{Q}$ and its derivatives $\partial\mathbf{Q}$, $F_{\mathrm{LdG}}(\mathbf{Q},\partial\mathbf{Q}) = \int_\Omega dV\,[f_b(\mathbf{Q}) + f_e(\partial\mathbf{Q}) + f_{q_0}(\partial\mathbf{Q})] + \int_{\partial\Omega} ds\, f_s(\mathbf{Q})$, with free-energy densities as [23,26–28]

$$f_b = \frac{2}{3}\tau\,\mathrm{Tr}\,\mathbf{Q}^2 - \frac{8}{3}\,\mathrm{Tr}\,\mathbf{Q}^3 + \frac{4}{9}(\mathrm{Tr}\,\mathbf{Q}^2)^2, \tag{1}$$

$$f_e = \frac{1}{3}(\partial_k Q_{ij})^2, \tag{2}$$

$$f_{q_0} = \frac{4q_0}{3} Q_{il}\epsilon_{ijk}\partial_j Q_{kl}. \tag{3}$$

Where Tr is the trace operator. The bulk free energy f_b describes the phase transition between the isotropic and the LC phases; the elastic contribution f_e is the same for nematics while f_{q_0} accounts for the spontaneous twist deformations observed in cholesteric phases. Here we adopt a dimensionless model and thus the free energy depends only on two bulk parameters τ and q_0, and length is measured in units of the correlation length ξ; as a reference, for a nematic such as the 5CB at room temperature $\xi \simeq 15$ nm. τ is a reduced temperature. Its value determines the equilibrium bulk phase. $q_0 = 2\pi/P_0$ is the inverse of the cholesteric pitch P_0. In this simple version of the Landau-de Gennes theory we allow for splay, twist, and bend deformations to have, in the limit of $P_0 \to \infty$ (the nematic limit), the same energy cost, also known as the one-elastic constant approximation. In nematics confined to toroidal domains it was found that the textures depend on the saddle-splay elastic constant K_{24}, which affects the surface orientation of the LC molecules and induces a twist on the nematic [18]. We assume this is not as relevant for cholesterics and choose to neglect this effect in the present work.

It is worth noting that the reduced temperature is, in reality, a function of qo and that the cholesteric-isotropic transition temperature depends on the (inverse) pitch of the cholesteric LC. Moreover, in the simplified form of Eq. (1) the coexistence temperature is always at $\tau_c = 1$. In this work we have set $\tau = 0.7\tau_c$.

To account for the presence of confining substrates, a surface free energy can be introduced. We restrict our study to substrates that impose parallel alignment of the nematic molecules. In particular, in the full three-dimensional problem (see below), we consider the Fournier-Galatola planar degenerate surface potential [29],

$$f_s = \frac{W}{2}\left[\mathrm{Tr}\,(\tilde{\mathbf{Q}} - \tilde{\mathbf{Q}}^\perp)^2 + \left(\mathrm{Tr}\,\tilde{\mathbf{Q}} - \frac{3}{2}S_s^2\right)^2\right], \tag{4}$$

where $W \simeq 10$ is the reduced surface anchoring constant, $\tilde{Q}_{ij} = Q_{ij} + S_s\delta_{ij}/2$ and $\tilde{\mathbf{Q}}^\perp = \mathbf{P}^T\tilde{\mathbf{Q}}\mathbf{P}$, with the projection matrix $P_{ij} = \delta_{ij} - \nu_i\nu_j$; $\vec{\nu}$ is the surface normal. The first term penalizes deviations of the director field from any (local) parallel orientation on the substrate. The second term forces the degree of orientational order to coincide with S_s, the preferred degree of orientational order at the surface. Here we consider that $S_s = S_b = (3/4)(1 + \sqrt{1 - 8\tau/9})$, where S_b is the equilibrium value of the bulk order parameter. In our 2D calculations we have assumed fixed-boundary conditions (strong anchoring limit) and forced the director to be either in- or off-plane.

In this work we address the effect of curvature on the cholesteric pitch. To that end we are interested in measuring the local pitch $P(\mathbf{r})$ that characterizes the local twist of the director field $\mathbf{n}$. This is done by evaluating the twist parameter [30,31] $S_{\mathrm{tw}} = \varepsilon_{ijk}Q_{il}\partial_j Q_{lk}$, which is inversely proportional to the pitch,

$$\frac{P(\mathbf{r})}{P_0} = -\frac{9}{4}\frac{S^2}{S_{\mathrm{tw}}}q_0. \tag{5}$$

The sign is related to the direction of rotation of the twist deformation. S_{tw} is negative if the rotation is anticlockwise and positive if clockwise.

This study was performed in different steps. We first considered cholesteric systems with either translational or cylindrical symmetry. This allows to simplify the problem to two dimensions (2D). Our 2D studies were performed with COMSOL 3.5a [32], which uses finite elements techniques to solve the Euler-Lagrange equations that follow from the minimization of the Landau-de Gennes free energy. Details on this method can be found in Ref. [33]. Finally, we considered the full three dimensional problem of toroidal droplets and minimized the free energy with finite element methods with adaptive meshing, described in detail in Ref. [34]. In both 2D and 3D studies our meshes are refined to ensure a numerical precision $< 1\%$ for the Landau-de Gennes free energy.

To investigate the presence of metastable states we have considered different initial conditions. Starting from the isotropic phase, corresponding to a fast quench, the cholesteric may be trapped in a texture with broken symmetry, at low pitch, which was found to be metastable. For flat and cylindrical walls (Secs. III A and III B) the global minimum was obtained by considering that the cholesteric is initially aligned with its layers parallel to the substrate. For cylindrical pores starting from an onion-like configuration, where the cholesteric "layers" are concentric, with uniform pitch P_0 was the best strategy to avoid metastable configurations. Finally, for toroidal domains the additional curvature guides the system to a unique state. We also considered initially a nematic perpendicular to the cross-section and found that the system converged to the same state.

III. RESULTS

A. Cholesteric near a flat surface

When a cholesteric phase is in contact with a flat substrate the anchoring on the surface forces the cholesteric LC to assume a preferred configuration. For example, if the surface induces planar anchoring, the cholesteric orients its twist axis in such a way that the cholesteric layers are aligned parallel to the substrate. If by any means the cholesteric were to align its twist axis parallel to the substrate, the orientational frustration

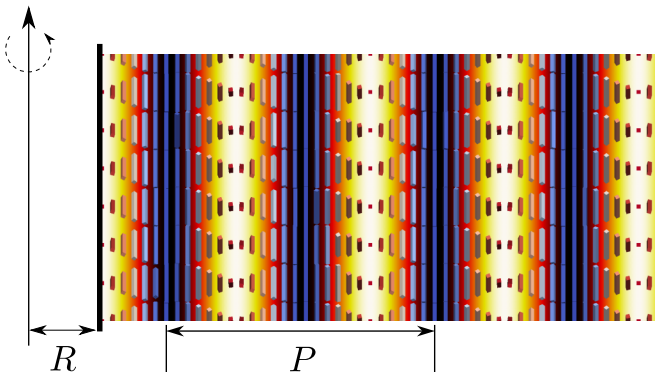

FIG. 1. Schematic of a cholesteric in contact with a wall (dark bar on the left) of curvature radius R. The pitch P is defined here as the distance needed for the orientational field to rotate by 2π. The configuration presented corresponds to the limit of a flat surface ($R \to \infty$). The color indicates the off-plane (angular, n_θ) component of the orientational field. White: the director points out of the plane; Black: the director is in-plane.

imposed by the surface anchoring would induce the nucleation of evenly spaced defects at the substrate, thus increasing the free energy of the system. Such configuration is only preferred if the anchoring on the substrate is homeotropic, as in that case there is no other configuration with lower energy cost [35]. Here we restrict our study to surfaces with planar anchoring.

In Fig. 1 we show the preferred configuration of a cholesteric LC near a flat wall (dark bar on the left) with planar anchoring. The cholesteric twists in the direction perpendicular to the substrate and forms a layer-like system. The phase is characterized by a twist pitch P, which is constant throughout the entire system and coincides with the natural cholesteric pitch P_0 that is an input to the model, and describes

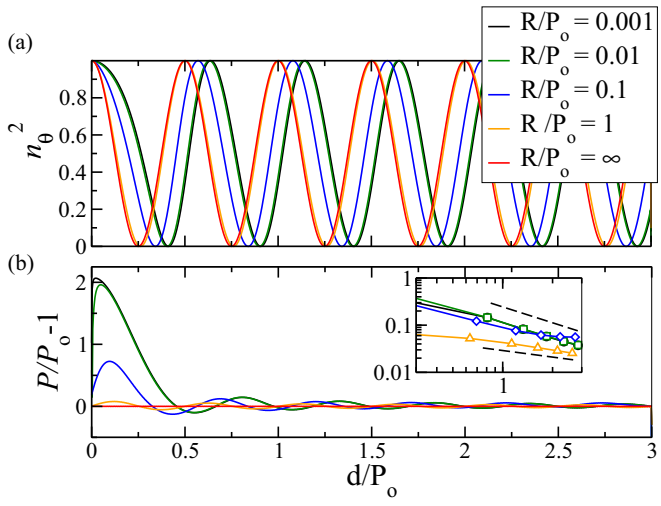

FIG. 2. (a) Square of the off-plane (angular) component of the director field n_θ^2 and (b) cholesteric pitch P as functions of the distance to the wall d with curvature radii $R/P_0 = 0.001, 0.01, 0.1, 1, \infty$. P_0 is the natural pitch of the system. In the inset: maxima of P as a function of the distance. The dashed lines correspond to $P/P_0 - 1 \sim (d/P_0)^{-\alpha}$ with $\alpha = 0.01, 0.05$ and are represented for comparison.

the undulation of the director field, shown in Fig. 2(a) for $R/P_0 = \infty$.

B. Adding curvature: From flat to cylindrical surfaces

To address the effect of curved surfaces we consider that the wall is the surface of a cylinder of radius R, as defined in Fig. 1. In this case the flat surface corresponds to the limit $R \to \infty$, for which the cholesteric "layers" are equally spaced by $P_0/2$. In Fig. 2(a) we show how the square of the off-plane director component n_θ^2 varies with the distance to the wall d for different radii $R/P_0 = 0.001, 0.01, 0.1, 1, \infty$. n_θ^2 is a harmonic function of the distance varying from 0 to 1. Clearly, if the radius of curvature is comparable to the natural pitch P_0 then n_θ^2 is very similar to the one obtain for the flat wall ($R/P_0 = \infty$). However, if the radius of curvature is much smaller than the pitch, Fig. 2(a) shows that n_θ^2 is shifted significantly and its maxima and minima occur farther away from the wall when compared with the flat case. This indicates that as the curvature increases (R decreases) the actual pitch of the cholesteric deviates from its natural value P_0.

Figure 2(b) shows how the local pitch P [defined in Eq. (5)] varies with the distance to the wall d for different radii $R/P_0 = 0.001, 0.01, 0.1, 1, \infty$. For the flat wall the pitch $P = P_0$ is constant everywhere, as already discussed. As the radius of the cylinder is decreased the local pitch P undulates close to the natural pitch value and converges to P_0 far from the wall $d \to \infty$. By increasing the curvature of the wall the undulations of P are more pronounced close to the substrate, but rapidly decay as d increases. However, for distances $d > 0.75P_0$ the decay is very slow as can be shown in the inset of Fig. 2(b). The points indicate the maxima of P and the dashed lines correspond to $P/P_0 - 1 \sim (d/P_0)^{-\alpha}$, where $\alpha = 0.01$ (bottom line) and $\alpha = 0.05$ (upper line).

The undulating behavior seen here is related to the compression $P < P_0$ and dilation $P > P_0$ of the cholesteric, and it comes from the energetic cost associated with a bend deformation induced by the cylindrical symmetry, allied with the cholesteric twist. For example, consider the cholesteric layer in which the off-plane component reaches zero. In this situation, the bending energy associated with bending such "layer" is nearly zero. However, the bending energy is large for the layers in which $n_\theta^2 = 1$. This indicates that the system can compromise between dilating the layers with $n_\theta = 0$ and compressing those with $n_\theta^2 = 1$.

To clarify this, we compare the pitch deviation, P/P_0, with the splay-bend parameter [23,27,31],

$$S_{\rm sb} = \frac{\partial^2 Q_{ij}}{\partial x_i \partial x_j}. \tag{6}$$

In Fig. 3 we plot the results for $P/P_0 = 0.001, 0.01, 0.1$. Clearly there is a strong correlation between P and $S_{\rm sb}$. When the local pitch P decreases $S_{\rm sb} < 0$, and when it increases $S_{\rm sb} > 0$. Additionaly, similar to P, the amplitude of $S_{\rm sb}$ decreases with increasing distance to the wall. The $S_{\rm sb}$ parameter is useful to identify regions of splay and bend. Since in the uniaxial case it can be rewritten as $S_{\rm sb} = (2S/3)\nabla \cdot [\mathbf{n}(\nabla \cdot \mathbf{n}) - \mathbf{n} \times (\nabla \times \mathbf{n})]$, the $S_{\rm sb} > 0$ regions are usually identified as splay regions and $S_{\rm sb} < 0$ as bend regions [23,27,31]. However, it turns out

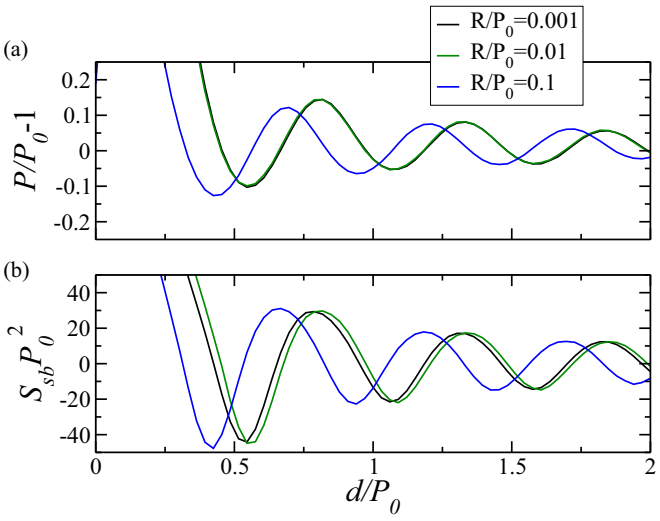

FIG. 3. Comparison between (a) the pitch deviations P/P_0 and (b) the splay-bend parameter S_{sb}, as functions of the distance to the wall d with curvature radii $R/P_0 = 0.001, 0.01, 0.1$.

that this is not always the case. To understand the values taken by $S_{\rm sb}$ consider a cholesteric with concentric "layers," e.g., $\mathbf{n} = [-\sin(q_0 d)y/d,\ \sin(q_0 d)x/d,\ \cos(q_0 d)]$, where $d = \sqrt{x^2 + y^2}$, with constant pitch P_0. Since $\nabla \cdot \mathbf{n} = 0$ there are no splay deformations. Only bend deformations contribute to $S_{\rm sb}$ and the splay-bend parameter becomes

$$S_{\rm sb} = \frac{2S}{3}\left[-q_0 \frac{\sin(2q_0 d)}{d}\right]. \tag{7}$$

This is a harmonic function with an amplitude that decays with $1/d$. This means that, even in the absence of splay deformations, $S_{\rm sb}$ can take positive values. It is thus clear that the changes in the local pitch occur as a response not only to bend deformations but specially to their variation. As shown in Fig. 3, as the bend deformations increase the local pitch decreases to reduce the size of those regions. Additionally, as the bend deformations decrease the cholesteric dilates, i.e., P increases. These effects are more pronounced in regions of strong curvature and decay as the distance to the wall d increases.

C. Cholesteric confined to cylinders

We now consider that the cholesteric is confined to a cylindrical tube of radius r. Such a system was previously studied by Ambrozic and Žumer [24,25]. Here, we restrict our study to configurations that have translational symmetry and consider two different orientations on the surface of the cylinder, shown in Figs. 4(a) and 4(b) for $r/P_0 = 1.25$: (i) $\mathbf{n}$ is along the symmetry axis of the cylinder, and (ii) the director is in-plane and parallel to the surface of the cylinder. In both cases the cholesteric twists radially forming an onion-like configuration. As we consider strong anchoring this type of configuration, also known as *radially twisted*, was predicted to be stable by Ambrozic and Žumer [24,25].

Figure 5 shows a cholesteric LC inside a long cylinder of radius $r = 500\xi$ for different pitch P_0 values and the same two types of boundary conditions shown in Fig. 4. In

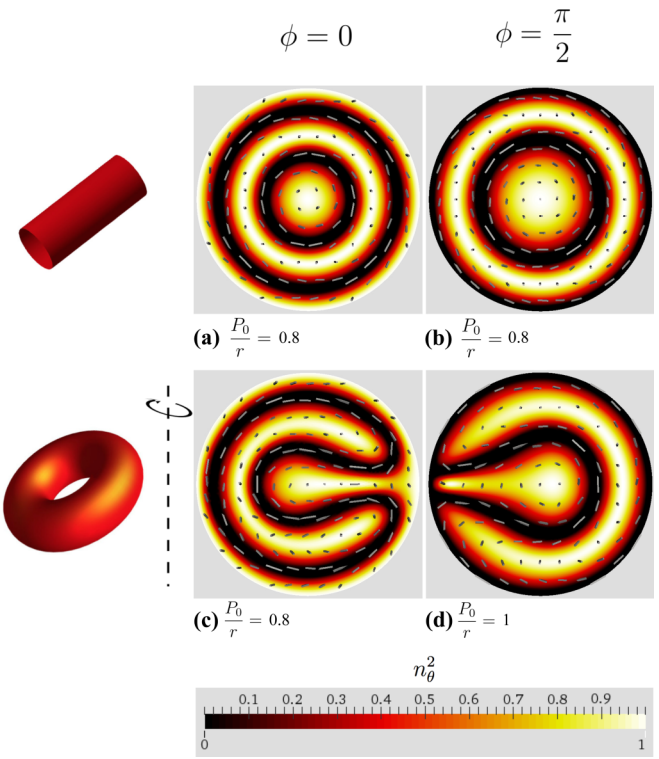

FIG. 4. Comparison between the cholesteric configurations for the no curvature limit [(a) and (b)] and for a curvature radius $R = 50\xi$ [(c) and (d)]. Systems (a) and (c) have boundary conditions with $\phi = 0$ and systems (b) and (d) have $\phi = \frac{\pi}{2}$. The color represents n_θ^2, the square of the component of the director along $\mathbf{e}_\theta$. The gray bars represent the director field.

the configurations found, the cholesteric at the center of the cylinder is always pointing off-plane. This means that when at the boundary the director is also off-plane, the cholesteric will try to perform (radially) at least a half turn [see Fig. 5(a)]. However, if the $\mathbf{n}$ at the surface of the cylinder is in-plane, the minimum rotation that the cholesteric can perform is $1/4$ of a turn [see Fig. 5(f)]. We have found that under these conditions the onion-like configuration is a global minimum and that for low values of the pitch $P_0 \leqslant 0.5r$ a metastable state with split cholesteric layers resembling the texture of finger-prints may occur.

In the bottom row of Fig. 5 we show the splay-bend parameter for the configurations with off-plane orientation at the boundary ($\phi = 0$). At the center of the cross-section the director is off-plane. As it moves away from the center it twists and its in-plane component increases, thus increasing the bend deformation (blue regions). After it is completely in-plane the director continues to twist now reducing the bend deformations (yellow regions) by decreasing its in-plane component. As discussed in the previous section this increase and the decrease in bend deformations induces the contraction and dilation of the concentric "layers," respectively.

For both orientations at the surface of the cylindrical pores, the cholesteric displays an onion-like configuration with the cholesteric layers arranged as concentric cylinders with a λ^{+1} nonsingular defect at the center [22,23]. Note that, for low values of the pitch $P_0 \leqslant 0.5r$ some of the layers may be

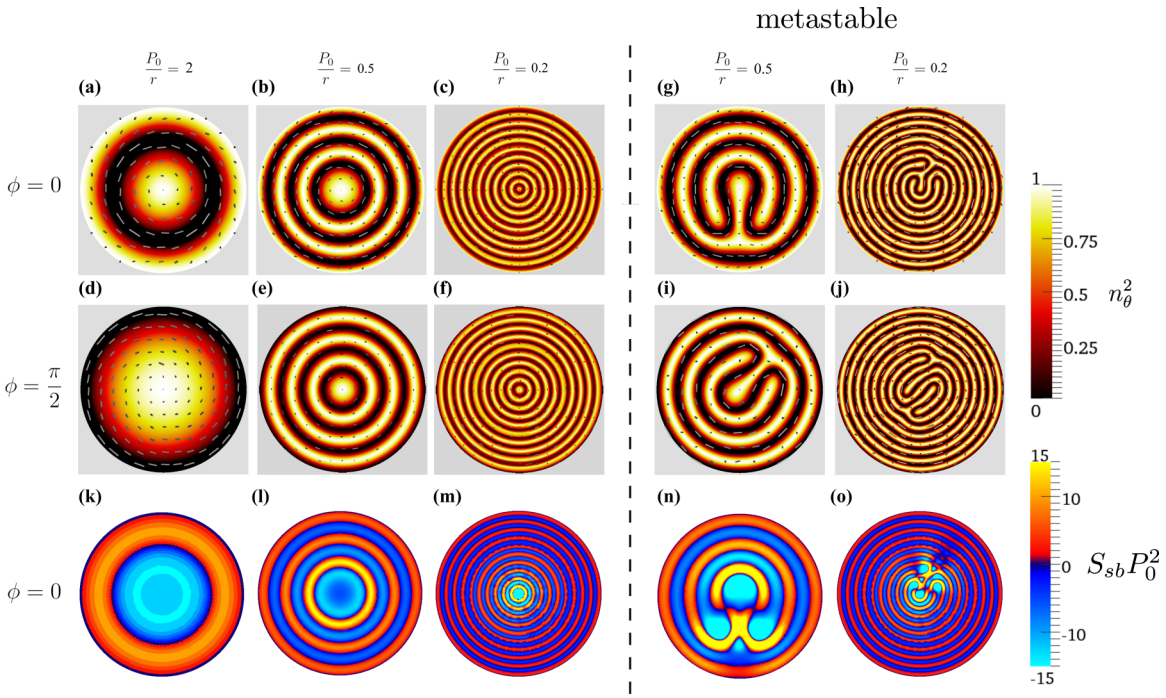

FIG. 5. Equilibrium configurations for a cholesteric liquid crystal inside an infinite cylinder with radius $r = 500\xi$ and $P_0/r = 2, 0.5, 0.2$. (a–c) Fixed boundary conditions with director parallel to the long axis of the cylinder. (d–f) Fixed boundary conditions with director tangent to the limiting circumference. The panels (g) and (h), (i) and (j) correspond to metastable states obtained, respectively, for off-plane and in-plane boundary conditions. The color represents n_θ^2, the off-plane component of the director. The gray bars represent the director field. In the bottom row (k–o) we represent the splay-bend parameter $S_{\rm sb}$ for the configurations in the top row. For better viewing and comparison we have restricted the splay-bend parameter to $-15 < S_{\rm sb}P_0^2 < 15$.

disrupted. In this metastable state, the system is trapped in a configuration with split cholesteric layers, particularly those closer to the center as it is there that the bending energy is higher. In this case the λ^{+1} nonsingular defect splits into two

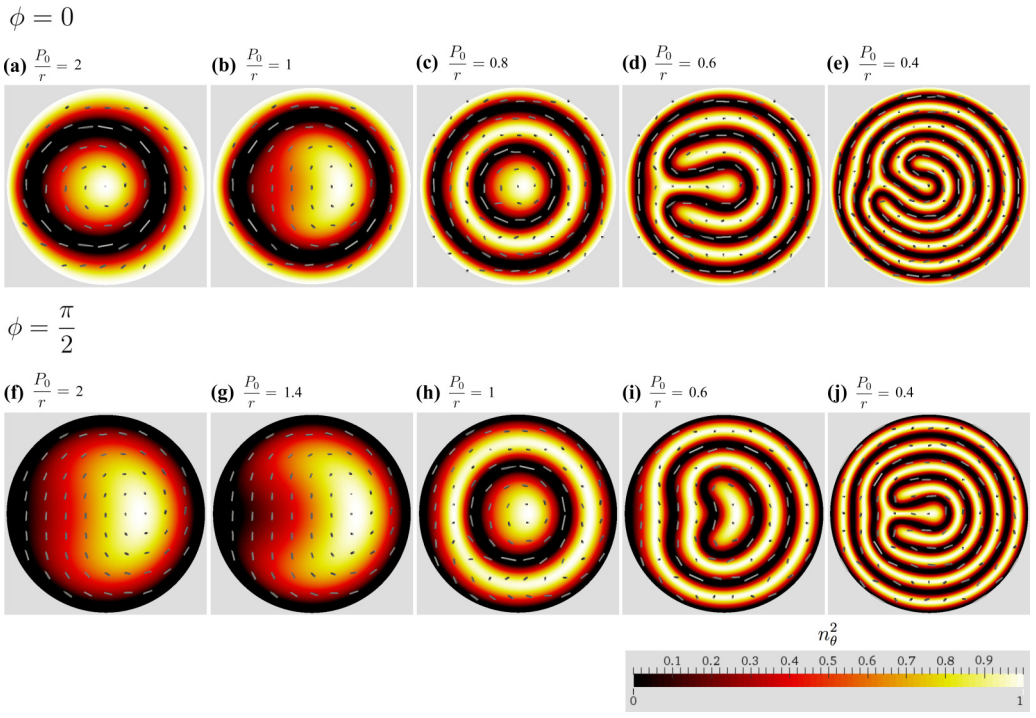

FIG. 6. Cholesteric configurations for a system with radius of curvature $R = 50\xi$ and cross-section $r = 500\xi$. Panels (a)–(e) correspond to boundary conditions with $\phi = 0$, and (f)–(j) have boundary conditions with $\phi = \frac{\pi}{2}$. The color represents n_θ^2, the square of the component of the director along $\mathbf{e}_\theta$. The gray bars represent the director field.

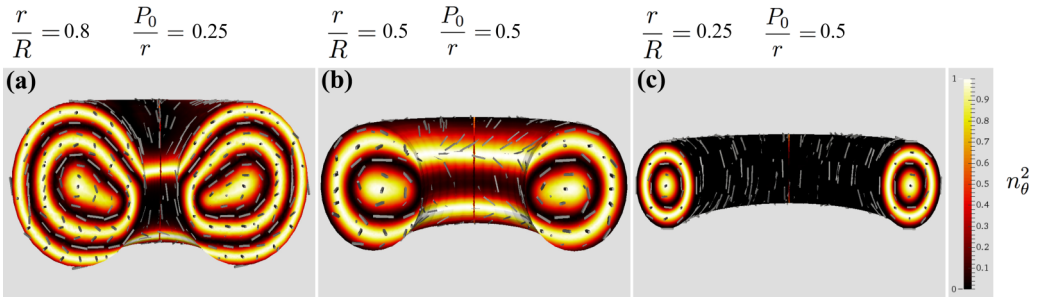

FIG. 7. Configurations of a cholesteric inside a torus, with multiple layers. (a) $\frac{r}{R} = 0.8, \frac{P_0}{r} = 0.25$, (b) $\frac{r}{R} = 0.5, \frac{P_0}{r} = 0.5$, (c) $\frac{r}{R} = 0.25, \frac{P_0}{r} = 0.5$. The color scale refers to n_θ^2 and the gray bars represent the director field.

$\lambda^{+1/2}$ and additional $\lambda^{+1/2}$–$\lambda^{-1/2}$ pairs appear. It is only in the torus, discussed in the next section, that this finger-print texture becomes a global minimum.

D. Full confinement: From a cylinder to a torus

Confining the cholestic LC inside a cylindrical pore clearly affects the local pitch, not only due to the curvature of the confining surface but also due to the competing length scales, the pitch P, and the radius of the cylinder r.

Within good approximation a torus (doughnut) of infinite principal radius, $R \to \infty$, corresponds to a long cylinder. This means that as the principal radius of the torus is decreased the cholesteric layers confined inside the torus should respond accordingly to the additional curvature as depicted in Figs. 4(c) and 4(d).

In Fig. 6 we show the cholesteric layers inside a torus of principal radius $R = 50\xi$ and cross-section $r = 500\xi$ for different pitch values P_0. Again, we consider two types of anchoring orientations at the surface of the torus: Figs. 6(a)–6(e) in-plane $\phi = 0$, and Figs. 6(f)–6(j) off-plane $\phi = \pi/2$. The (cylindrical) symmetry axis is located on the left. As in Sec. III B, when the director is parallel to the symmetry axis there is no additional bending energy associated to extending that particular region, and whenever the director is perpendicular to the symmetry axis (off-plane) it is preferable to contract that region to reduce bend deformations. As a result, even for the case of concentric layers in the $R \to \infty$ limit the layers are deformed.

As in the case of a cylindrical pore, when the pitch is small $P_0 \leqslant 0.5r$, the central layers are allowed to break allowing the outer layers to extend toward the center of the cross-section. Here this configuration is a global minimum and the extension of the outer layers is along the equatorial plane of the torus, indicating that there is a constraint on this extension set by the additional curvature.

Finally, we considered the full 3D problem. Figure 7 shows the configuration of cholesteric LCs confined to toroidal droplets with planar degenerate anchoring; i.e., here the LC molecules are allowed to align in any direction parallel to the surface of the torus. As a result, the cholesteric is now able to relieve some of the built-in stress due to the curved surface that confines it by taking different orientations around the same cross-section. As such, the cholesteric exhibits broken layers that penetrate the surface. We note that on the equatorial plane, in the inner most region of the surface of the torus, where the curvature is highest, the director field is parallel to the symmetry axis, thus preventing an increase in the free energy of the system through bend deformations.

IV. CONCLUSIONS

In this manuscript we have considered the effect of curvature on the pitch of a cholesteric liquid crystal. We started by considering a cholesteric LC in contact with a cylindrical wall of a given radius. We found that, because of the curvature, the cholesteric is subjected to additional bend distortions that influence the orientational field. As a result, the cholesteric contracts the regions where this bend deformation is higher and dilates the ones where it is lower, thus changing locally the value of the pitch P. These distortions were found to be larger for higher curvatures (thinner cylinders) but rapidly decaying with the distance to the wall.

When the cholesteric is inside a cylindrical pore the distortion effect due to the curvature of the confining wall is again present. Typically, the cholesteric takes an onion-like configuration with the cholesteric "layers" adopting the form of concentric cylinders. However, if the radius of the cylinder is larger than the natural cholesteric pitch, $P_0/r \leqslant 0.5$, the stress from the bend deformations drives the inner most layers to split and the cholesteric takes a configuration resembling that of finger prints. However, we found that for the range of parameters that were investigated, the "finger-print" configuration is always metastable for the cylindrical pore.

We then considered the cholesteric to be confined in a toroidal droplet, with cylindrical symmetry around its symmetry axis. For an infinitely large torus the cholesteric adopts the same configurations as in the cylindrical confinement case with a given cross-sectional radius. As the torus is made smaller there is a shift in the position of the cholesteric layers that appears as a result of the additional curvature. The effect is more pronounced for smaller radii, where some cholesteric layers split close to the symmetry axis and the cholesteric takes the finger-print texture.

Finally, we considered the full three-dimensional toroidal droplet and assumed planar degenerate anchoring on the surface of the torus. We corroborate the results found for systems with cylindrical symmetry. Particularly, we found that the distortion of the natural pitch depends heavily on the

curvature of the droplet. However, because the system is less constrained, particularly at the confining surface, we observe an enhancement of the splitting of the cholesteric layers. It is only in this case where the LC molecules were allowed to choose their optimal orientation that the saddle-splay elastic constant could have an effect.

Our main conclusion is that the curvature, and in particular that of the toroidal droplets, affects the local orientation of the cholesteric LC distorting the periodicity of the spontaneous twist deformation. For the case of confining surfaces, this results in a symmetry breaking of the cholesteric layers that depends not only on the curvature of the bounding surface but also on the pitch and the geometrical parameters.

As a final note, experiments on cholesteric phases of suspensions of virus reported that the pitch decreases as a power law of the virus concentration [36,37]. Our results indicate that in the presence of curved confining surfaces the local pitch undulates leading to a nonhomogeneous concentration of virus in such suspensions.

ACKNOWLEDGMENTS

We acknowledge the financial support of the Portuguese Foundation for Science and Technology (FCT) under Contracts No. UID/FIS/00618/2013 and No. EXCEL/FIS-NAN/0083/2012.

[1] J. A. Castellano, *The Story of Liquid Crystal Displays and the Creation of an Industry* (World Scientific, Singapore, 2005).
[2] C. Hilsum, Phil. Trans. R. Soc. A **368**, 1027 (2010).
[3] Y. S. Choi, J. U. Yun, and S. E. Park, J. Non-Cryst. Solids **431**, 2 (2016).
[4] T. Scheffer and J. Nehring, Appl. Phys. Lett. **45**, 1021 (1984).
[5] K. Tarumi, M. Heckmeier, and M. Klasen-Memmer, J. Soc. Inf. Disp. **10**, 127 (2002).
[6] J. W. Doane, A. Golemme, J. L. West, J. B. Whitehead Jr., and B.-G. Wu, Mol. Cryst. Liq. Cryst. **165**, 511 (1988).
[7] H.-S. Kitzerow, Liq. Cryst. **16**, 1 (1994).
[8] P. Drzaic and P. S. Drzaic, Liq. Cryst. **33**, 1281 (2006).
[9] P. G. de Gennes and J. Prost, *The Physics of Liquid Crystals*, 2nd ed (Claredon, Oxford, 1993).
[10] P. M. Chaikin and T. C. Lubensky, *Principles of Condensed Matter Physics* (Cambridge University Press, Cambridge, UK, 1995).
[11] P. Patrício, J. M. Romero-Enrique, N. M. Silvestre, N. R. Bernardino, and M. M. Telo da Gama, Mol. Phys. **109**, 1067 (2011).
[12] H. Stark, Phys. Rep. **351**, 387 (2001).
[13] J. P. Xu and W. J. Li, in *3rd International Conferences on Consumer Electronics, Communications and Networks (CECNET)* (IEEE, 2013), pp. 250–253.
[14] M. A. White and M. LeBlanc, J. Chem. Educ. **76**, 1201 (1999).
[15] Y. Jiang, R. Wilson, A. Hochbaum, and J. Carter, Proc. SPIE **4677**, 247 (2002).
[16] E. Montbach, M. Lightfoot, and J. Doane, Inductive switching of cholesteric liquid crystal display device (2016), U.S. Patent 9 235 096.
[17] M. G. Campbell, M. Tasinkevych, and I. I. Smalyukh, Phys. Rev. Lett. **112**, 197801 (2014).
[18] E. Pairam, J. Vallamkondu, V. Koning, B. C. van Zuiden, P. W. Ellis, M. A. Bates, V. Vitelli, and A. Fernandez-Nieves, Proc. Natl. Acad. Sci. USA **110**, 9295 (2013).
[19] V. M. O. Batista, N. M. Silvestre, and M. M. Telo da Gama, Phys. Rev. E **92**, 062507 (2015).
[20] Y. Geng, P. L. Almeida, J. L. Figueirinhas, E. M. Terentjev, and M. H. Godinho, Soft Matter **8**, 3634 (2012).
[21] Y. Geng, D. Sec, P. L. Almeida, O. D. Lavrentovich, S. Zumer, and M. H. Godinho, Soft Matter **9**, 7928 (2013).
[22] M. Kleman and O. D. Lavrentovich, *Soft Matter Physics: An Introduction* (Springer-Verlag, Berlin, 2001).
[23] D. Seč, T. Porenta, M. Ravnik, and S. Žumer, Soft Matter **8**, 11982 (2012).
[24] M. Ambrozic and S. Zumer, Phys. Rev. E **54**, 5187 (1996).
[25] M. Ambrozic and S. Zumer, Phys. Rev. E **59**, 4153 (1999).
[26] M. Ravnik, G. P. Alexander, J. M. Yeomans, and S. Žumer, Faraday Discuss. **144**, 159 (2009).
[27] S. Čopar, T. Porenta, and S. Žumer, Phys. Rev. E **84**, 051702 (2011).
[28] N. R. Bernardino, M. C. F. Pereira, N. M. Silvestre, and M. M. T. da Gama, Soft Matter **10**, 9399 (2014).
[29] J.-B. Fournier and P. Galatola, Europhys. Lett. **72**, 403 (2005).
[30] A. Kilian and A. Sonnet, Z. Naturforsch. A **50**, 911 (1995).
[31] S. Čopar, T. Porenta, and S. Žumer, Liq. Cryst. **40**, 1759 (2013).
[32] I. COMSOL, *COMSOL Multiphysics, Version 3.5a User's Guide* (COMSOL, Inc., Burlington, MA, 2005).
[33] A. R. A. da Luz Fialho, Msc thesis, Universidade de Lisboa, 2015.
[34] M. Tasinkevych, N. M. Silvestre, and M. M. T. da Gama, New J. Phys. **14**, 073030 (2012).
[35] N. M. Silvestre, M. C. F. Pereira, N. R. Bernardino, and M. M. T. da Gama, Eur. Phys. J. E **39**, 13 (2016).
[36] Z. Dogic and S. Fraden, Langmuir **16**, 7820 (2000).
[37] E. Barry, D. Beller, and Z. Dogic, Soft Matter **5**, 2563 (2009).